240 GHz electron paramagnetic resonance studies of intrinsic defects in as-grown 4*H* SiC

Valery V. Konovalov* and Mary Ellen Zvanut
Department of Physics, University of Alabama at Birmingham, Birmingham, Alabama 35294-1170, USA

Johan van Tol
Center for Interdisciplinary Magnetic Resonance, National High Magnetic Field Laboratory, Tallahassee, Florida 32310, USA
(Received 3 February 2003; published 2 July 2003)

240 GHz electron paramagnetic resonance (EPR) measurements of as-grown nominally semi-insulating 4*H* SiC detected two well-separated centers ID1 and ID2. The EPR parameters of ID1 and ID2 coincide with that of EI5 and EI6 centers previously detected in 2-MeV electron-irradiated *p*-type 4*H* SiC:Al by 95 GHz EPR (Son *et al.*). The defects in irradiated material were assigned to a positively charged carbon vacancy (EI5) and silicon antisite (EI6), respectively. Increased separation between the two centers at 240 GHz and the absence of additional radiation-induced spectral lines in the as-grown, unirradiated SiC facilitated analysis of the defect structure. Our data support that the ID1 center is a carbon vacancy-related defect, but is not consistent with the assignment of the ID2 center to a silicon antisite. The ID2 spectrum is best fit as another carbon vacancy-related defect. Illumination with light below 1400 nm quenched both ID1 and ID2 simultaneously, suggesting that the defect energy levels are nearly the same.

DOI: 10.1103/PhysRevB.68.012102 PACS number(s): 61.72.Hh

Intrinsic defects have been studied intensively in SiC,[1–14] which is a popular wide-band-gap material for high-power and high-temperature microelectronics.[15] Recently, deep-level intrinsic defects have attracted considerable interest as potential electron-hole traps suitable for compensation of residual impurities in high-quality SiC.[16] The presence of a deep intrinsic defect (ID) capable of exchanging charge with boron-nitrogen impurities has been demonstrated by *X*-band ($\sim$9.5 GHz) electron paramagnetic resonance (EPR) in as-grown nominally semi-insulating 4*H* SiC produced by Cree Inc. with vanadium-free technology.[13,14] The *X*-band EPR spectrum of ID consists of two barely resolved lines ID1 and ID2. These coincide with the *X*-band spectra of EI5/EI6 and Ky2/Ky3 centers detected in 2-MeV electron-irradiated *p*-type 4*H*, 6*H* SiC:Al (Refs. 7–9) and 6*H* SiC:B (Refs. 11 and 12), respectively. Higher frequency *W*-band (95 GHz) EPR resolved EI5 and EI6 centers, which were assigned to a positively charged carbon vacancy and silicon antisite, respectively.[7–10] The assignment of each center was based on the analysis of the intensities of hyperfine (HF) satellite lines originating from the interaction of an electron spin ($S=1/2$) with a ^{29}Si magnetic nuclei ($I=1/2$). At the same time, density functional theory (DFT) calculations using small 4*H* SiC clusters suggested that EI5/Ky2 and EI6/Ky3 centers may represent two positively charged carbon vacancies at the quasicubic and hexagonal lattice sites of 4*H* SiC.[17] In this report, we present 240 GHz EPR measurements of the intrinsic defects in as-grown high-purity 4*H* SiC. Using a microwave frequency of 240 GHz, the ID1 and ID2 centers were well resolved, and it was determined that their EPR parameters are the same as those of EI5 and EI6 obtained at 95 GHz. The well-separated spectral lines combined with the lack of additional radiation-induced signals facilitated analysis of the defect structure.

High-purity as-grown nominally semi-insulating (0001) 4*H* SiC wafers, grown by the seeded sublimation method and provided by Cree Inc., were studied. Samples were kept in the dark in the EPR cavity at 294 K for 12 h prior to measurement. EPR spectra were recorded using an *X*-band Bruker ESR200 spectrometer and a 240 GHz spectrometer at the National High Magnetic Field Laboratory. The latter, a superheterodyne spectrometer, employed a quasioptical submillimeter bridge and operated in reflection mode without cavity. The incident power on the sample was about 20 μW. The magnetic field was calibrated using two standards: Si:P [$g=1.99850(2)$] and BDPA in polystyrene [$g=2.00250(2)$]. The BDPA and Si:P data agree very well with each other. The experimental design of the 240 GHz spectrometer did not allow sample rotation: thus only one sample orientation, $\mathbf{B}\|c$ axis was measured. EPR spectra were simulated with WINEPR SimFonia (Bruker Inc.) program.

Figure 1 shows the 9.75 GHz and 240 GHz EPR spectra of 4*H* SiC recorded in the dark at 77 K. The ID1 and ID2 centers, which are barely resolved at 9.75 GHz, became well separated at 240 GHz. The spectrum of each center consists of an intense central line and several satellite lines. The satellite lines can be categorized into a number of doublets, each assigned to particular central line according to the coincidence of doublet median and central line magnetic fields. The fact that separation between the doublets remains the same and positioned about the same central line at two EPR frequencies supports their assignment to the HF interactions with magnetic nuclei having spin $I=1/2$. For each center, the HF doublets at two EPR frequencies correspond well except for a mixing of the ID1-3 and ID1-4 doublets at 240 GHz due to the broader line width at higher frequency. The EPR parameters of ID1 and ID2 centers at 77 K are shown in Table I and are similar to the reported parameters of EI5 and EI6 centers.[7–10] In addition, we identified several new doublets with smaller HF constants, which where assigned to the ID1 and ID2 centers based on their similar *g* values.

EPR spectra of the ID1 and ID2 centers demonstrated a temperature dependence similar to that observed for the EI5 and EI6 centers, except that the ID1 center did not disappear below 25 K, as was reported for the EI5 center,[7,8] but rather

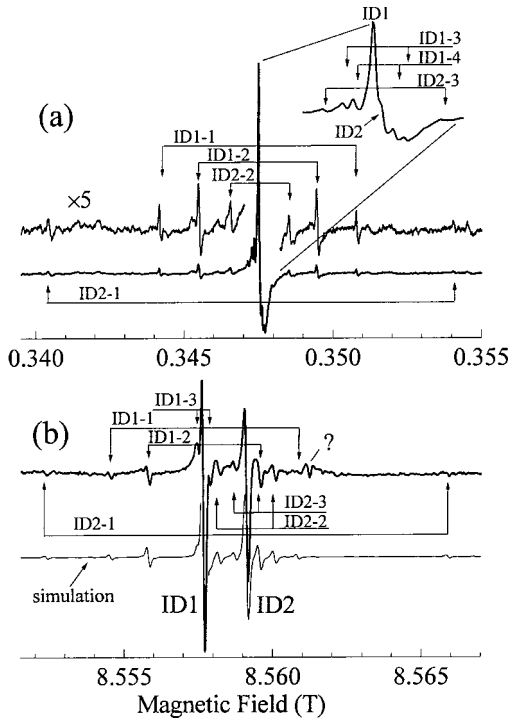

FIG. 1. 9.75 GHz (a) and 240 GHz (b) EPR spectra of 4*H* SiC recorded at 77 K. $\mathbf{B}\|c$ axis. The smooth thin line (b) is the simulated spectrum.

the intensity was reduced and the shape changed. The 240 GHz spectra of ID1 and ID2 at 10 K are shown in Fig. 2, and the temperature dependence of $g_{\|}$ is shown in Fig. 3. Table I lists the EPR parameters at 10 K and 77 K for each center. As the temperature increased from 4 K to 160 K, the $g_{\|}$ value for ID1 remained almost constant, but $g_{\|}$ for ID2 increased from 2.002 38 to 2.002 87. In the same temperature range, the intensity of ID1 decreased while that of ID2 increased. We observed that at temperatures below 70 K each ID1 line separated into two, while the ID2 lines remain unchanged. As seen in Table I, the EPR parameters of the centers did not depend strongly on the temperature, suggesting that the defect structure remained practically unaltered. The splitting of ID1 lines at lower temperature suggests that the electron spin density is localized on two energetically close structures of ID1 at low temperature and averaged between them at high temperature.

Individual HF satellite lines of each center can be assigned to particular magnetic nuclei using the ratios of central to satellite line intensities and the natural abundance of magnetic isotopes ^{29}Si (4.67%) and ^{13}C (1.11%).[1–13] The results of the assignments are shown in Table I. The EPR spectra simulated with parameters from Table I are shown in Fig. 1 (77 K) and Fig. 2 (10 K). Similar to what was reported for the IE5 center,[7,8] the two doublets of the ID1 center with the largest HF constants, ID1-1 and ID1-2, are assigned to $1\times^{29}$Si and $3\times^{29}$Si atoms, respectively. Assuming that they originate from nearest-neighbor (NN) HF interactions, the ID1/EI5 center may be ascribed to a carbon vacancy deformed along the *c* axis.[7,8,13] For the ID2 center the doublet with largest HF constant, ID2-1, is assigned to one ^{29}Si atom, in agreement with that determined for IE6.[7,9] However, our identification of the two doublets ID2-2 and ID2-3 differs from that reported for the EI6 center.[7,9] The intensities of ID2-2 and ID2-3 doublets were simulated best using two sets of $3\times^{29}$Si atoms or two sets of $12\times^{13}$C atoms, or a combination of each. Note that within a conventional EPR instrumental error of $\pm 5\%$, it is practically impossible to distinguish whether one ^{29}Si atom (4.67% abundance) or four ^{13}C atoms (4.44%) contribute to the HF line intensity. In contrast, the total intensity of the analogous doublets of the EI6 center, which we estimated from the SHF structure of the HF line with at $A_{\|}=138$ G [see Fig. 1(b) and Fig. 4 of Ref. 9], must represent two sets of $2\times^{29}$Si atoms. In addition, we have identified two doublets ID2-4 and ID2-5 not previously reported. The ID2-4 and ID2-5 doublets were assigned to $2\times^{13}$C and $3\times^{13}$C atoms, respectively. Based on the calculated number of ^{29}Si atoms for EI6 represented by each line of the HF structure ($1+2+2$ for the 3 lines at $\mathbf{B}\|c$ axis and $1+2+1+1$ for the 4 lines at $\mathbf{B}\perp c$ axis), Son *et al.*[9] suggested that this center is a silicon antisite defect. They assumed that one Si atom belongs to the central atom of the antisite and four others belong to NN Si atoms. Our 240 GHz data indicate that a different number of Si atoms participate in the ID2/EI6 center: thus they do not support the Si antisite model proposed earlier. In fact, the relative intensities for the SHF lines in Fig. 1(b) and Fig. 4 of Ref. 9 also contradict the assignment of the lines to a Si antisite defect. For an antisite, the SHF line intensity due to the neighboring Si atoms should be distributed in a 3:1 ratio when the magnetic field is parallel to the *c* axis. Instead, the spectrum consists of two pairs of lines of equal intensity. The relative amplitudes of these two pairs are identical to that measured at 240 GHz for ID2-2 and ID2-3 HF doublets. At present, it is not clear why the total intensities of ID2-2 and ID2-3 doublets relative to the central line differ from the corresponding doublets of EI6. Although the preparation of our high-purity as-grown SiC sample and electron-irradiated *p*-type samples containing about 10^{17} cm^{-3} Al was different, the EPR parameters of both defects ID2 and EI6 coincide well. One possible reason for the difference may be the presence of additional EPR lines from other defects observed in electron-irradiated SiC. Such lines are absent in our as-grown SiC. Note that in our spectra, the increased separation of the spectral lines at 240 GHz minimizes the accidental coincidence of different lines.

In the case of the ID1/EI5 center, two HF constants (ID1-1 and ID1-2) significantly exceed the others; thus the assumption that these lines are from the NN Si atoms is reasonable. Their intensity ratio is 1:3, which corresponds well to a carbon vacancy-related defect deformed along the *c* axis.[7,8,13] The ID1-3 and ID1-4 lines may be due to the second- and third-shell atoms.[13] For ID2/EI6, only the HF constant for ID2-1 differs significantly from the rest; therefore, it is difficult to attribute the remaining HF doublets to close or distant atoms. From our data, several structures of the ID2/EI6 defect may be suggested. One possibility is that it is an another carbon vacancy defect: NN are $1\times^{29}$Si (ID2-1) and $3\times^{29}$Si (ID2-2), NNN are $12\times^{13}$C (ID2-3), and more remote atoms are $2\times^{13}$C (ID2-4) and $3\times^{13}$C (ID2-5). Thus, ID1 and ID2 may represent a carbon vacancy defect at cubic and hexagonal lattice sites, as has been suggested in

TABLE I. EPR parameters of the ID1 and ID2 centers in 4*H* SiC at 77 K and 10 K[a] (in parentheses).

Center		Frequency (GHz)	$g_{\parallel}$	$A_{\parallel}$ (G)	Assignments
ID1	ID1-1	9.75	2.0031	66.4	$1\times{}^{29}$Si
	ID1-2			39.74	$3\times{}^{29}$Si
	ID1-3			4.24	$6\times{}^{13}$C
	ID1-4			2.78	$12\times{}^{13}$C or $3\times{}^{29}$Si
	ID1-1	240	2.00308	63.5 (63)	$1\times{}^{29}$Si
	ID1-2		(2.00313)	37.5 (38.5)	$3\times{}^{29}$Si
	ID1-3′			3.6 (3.5)	$12\times{}^{13}$C or $3\times{}^{29}$Si
ID2	ID2-1	9.75	2.0027	140.1	$1\times{}^{29}$Si
	ID2-2			19.6	$3\times{}^{29}$Si
	ID2-3			8.08	$12\times{}^{13}$C or $3\times{}^{29}$Si
	ID2-1	240.0	2.00273	135.1 (151.7)	$1\times{}^{29}$Si
	ID2-2		(2.00238)	18.63 (13.55)	$3\times{}^{29}$Si
	ID2-3			7.8 (8.45)	$12\times{}^{13}$C or $3\times{}^{29}$Si
	ID2-4			(26.5)	$2\times{}^{13}$C
	ID2-5			(5.5)	$3\times{}^{13}$C
		9.48	2.00322	64.6	$1\times{}^{29}$Si
EI5[b]				38.0	$3\times{}^{29}$Si
		94.89	2.00322	64.6	$1\times{}^{29}$Si
				38.0	$3\times{}^{29}$Si
		9.48	2.00302	138 (151)	$1\times{}^{29}$Si
EI6[c]				17 (15)[d]	$2\times{}^{29}$Si[b]
				8 (8)[d]	$2\times{}^{29}$Si[b]
		94.9	2.00302	138 (151)	$1\times{}^{29}$Si
			(2.00242)	17 (15)	$2\times{}^{29}$Si
				8 (8)	$2\times{}^{29}$Si

[a]For EI5 and EI6 the values were obtained at 138 K and 23 K (in parentheses) (Refs. 7 and 9).
[b]References 7 and 8.
[c]References 7 and 9.
[d]The $A_{\parallel}$ HF constants and number of magnetic nuclei for EI6 were estimated from the superhyperfine lines (SHF's) of the HF line with largest HF constant.

Refs. 11 and 12. Other structures may include substitutional impurities, interstitials, or complex defects such as impurity-impurity pair, divacancy, or vacancy-impurity pair. The interstitials may be excluded due to the high thermal stability of both ID1 and ID2 in as-grown SiC.[13] Isolated substitutional impurities are also unlikely because of the high purity of SiC used in the present work. Note that similar EPR spectra ID1/EI5/Ky2 and ID2/EI6/Ky3 are reported in a wide variety of SiC samples, including *p*-type 4*H*, 6*H* SiC:Al,[7–9] *p*-type 6*H* SiC:B,[11,12] and as-grown nominally semi-insulating 4*H* SiC.[10,13,14] The recurrence of these spectra in diverse samples indicates that the centers are not affected by a large variation of Al or B concentrations. Nevertheless, such complex defects as B(Al)-N pair, carbon vacancy-impurity (B,N) pair, and divacancy cannot be excluded because the concentration of those defects may not depend significantly on the variation of Al(B) concentration in *p*-type samples. Although we do not observe any HF lines attributable to B or N nuclei in the ID1 and ID2 spectra, we cannot exclude their presence. It is known that the electron spin density on the impurity atom with nuclear spin $I>1/2$ may be negligibly small and may not result in detectable HF splitting.[18,19] Recently, DFT calculations of 3C SiC demonstrated that $B_{Si}-V_C$ and B_C

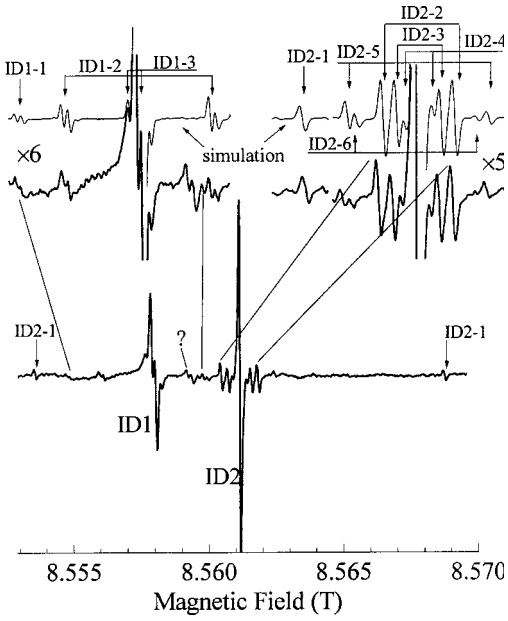

FIG. 2. 240 GHz EPR spectrum of 4*H* SiC recorded at 10 K. **B**$\|c$ axis. Smooth thin lines are the simulated spectra.

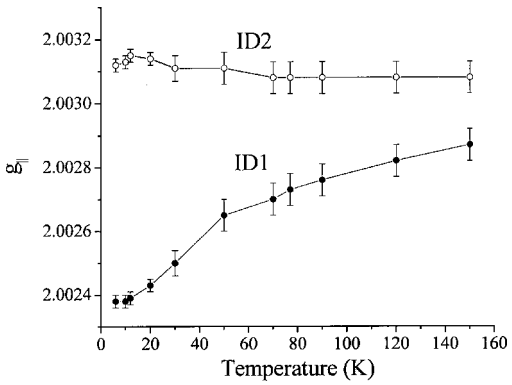

FIG. 3. Temperature dependence of $g_{\|}$ for ID1 (open circle) and ID2 (filled circle). Below 70 K, the ID2 lines separated and $g_{\|}$ was calculated from the median.

$-V_C$ complexes have low formation energies in SiC and should be present in high concentrations.[20] Furthermore, calculations demonstrated that those complexes have a carbon-vacancy-like electronic structure with only small contribution from boron orbitals. In our opinion, those boron-vacancy complexes could be candidates for ID1/EI5/Ky2 and ID2/EI6/Ky3 intrinsic defects. An ultimate analysis of the defect's electronic structure should include electron-nuclear double-resonance or electron spin-echo measurements, which are sensitive to HF interactions of electron spin with remote magnetic nuclei. The low concentration of the ID1/ID2 centers in as-grown SiC ($\sim 10^{14}$ cm^{-3}) did not allow such measurements at the *X*-band frequency, but we plan to realize them later using more sensitive high-field EPR.

The dependence of photoinduced *X*-band EPR signals on photon energy has been used to locate the energy level of the ID1/ID2 defect with respect to the band edges.[14] In earlier work, illumination with sub-band-gap light quenched the ID1/ID2 signals. However, since only the change of the central line intensity at 4.2 K was monitored, the ID1 and ID2 intensities could not be distinguished. Here we discuss results of *X*-band photo-EPR measurements of satellite lines, ID1-1,2 and ID2-3, at 77 K where both ID1 and ID2 can be monitored. The data demonstrate that the intensity of both ID1 and ID2 centers starts to decrease simultaneously at about 1400 nm, indicating that defects have about the same energy levels. The nearly equal levels of the two defects favors a model based on a carbon vacancy-related defect located at the cubic and hexagonal lattice sites of SiC, which likely are energetically close. Recent DFT and local spin density approximation (LSDA) calculations predict that the difference between ionization levels for a carbon vacancy at cubic and hexagonal sites in 4*H* SiC is within 0.2 eV.[21,22] For example, the energy of $(0/+)$ level, which most probably corresponds to the observed defects, is 1.37 (cub) and 1.44 eV (hex),[21] or 1.22 (cub) and 1.34 eV (hex),[22] with respect to the valence band edge (E_V). On the other hand, DFT predicts only one shallow acceptor level for a silicon antisite, $E_V+0.2$ eV.[22]

High-field 240 GHz EPR measurements of as-grown nominally semi-insulating 4*H* SiC revealed two centers, ID1 and ID2. The EPR parameters of ID1 and ID2 coincide with those of EI5 and EI6 detected previously at 95 GHz in 2-MeV electron-irradiated *p*-type 4*H* SiC:Al and assigned to a positively charged carbon vacancy and silicon antisite, respectively.[9,12] Our 240 GHz data support that ID1/EI5 center is a carbon vacancy-related defect, but is not consistent with the assignment of the ID2/EI6 center to a silicon antisite. ID2 could be a carbon vacancy-related defect situated at a different lattice site of 4*H* SiC than ID1 or a complex defect such as a V_C-B pair. Illumination below 1400 nm quenched both ID1 and ID2 simultaneously, indicating that both defects have nearly the same energy levels.

The work at UAB was supported by Dr. Colin Wood through a grant from the Office of Naval Research.

*Electronic address: vkono@uab.edu.

[1] L. A. S. Balona and J. H. N. Loubster, J. Phys. C **3**, 2344 (1970).
[2] J. Schneider and K. Maier, Physica B **185**, 199 (1993).
[3] H. Itoh, A. Kawasuso, T. Ohshima, M. Yoshikawa, I. Nashiyama, S. Tanigawa, S. Misawa, H. Okumura, and S. Yoshida, Phys. Status Solidi A **162**, 173 (1997).
[4] P. G. Baranov, Defect Diffus. Forum **148–149**, 129 (1997).
[5] A. A. Lebedev, Semiconductors **33**, 107 (1999).
[6] E. N. Kalabukhova, S. N. Lukin, A. Saxler, W. C. Mitchel, S. R. Smith, and J. S. Solomon, Phys. Rev. B **64**, 235202 (2001).
[7] N. T. Son, P. N. Hai, and E. Jansen, Mater. Sci. Forum **353–356**, 499 (2001).
[8] N. T. Son, P. N. Hai, and E. Jansen, Phys. Rev. B **63**, 201201 (2001).
[9] N. T. Son, P. N. Hai, and E. Jansen, Phys. Rev. Lett. **87**, 045502 (2001).
[10] N. T. Son, B. Magnuson, Z. Zolnai, A. Ellison, and E. Jansen, Mater. Sci. Forum **433–436**, 45 (2003).
[11] V. Y. Bratus, I. N. Makeeva, S. M. Okulov, T. L. Petrenko, T. T. Petrenko, and H. J. von Bardeleben, Mater. Sci. Forum **353–356**, 517 (2001).
[12] V. Y. Bratus, I. N. Makeeva, S. M. Okulov, T. L. Petrenko, T. T. Petrenko, and H. J. von Bardeleben, Physica B **308–310**, 621 (2001).
[13] V. V. Konovalov, M. E. Zvanut, V. F. Tsvetkov, J. R. Jenny, S. G. Müller, and H. McD. Hobgood, Physica B **308–310**, 631 (2001).
[14] M. E. Zvanut and V. V. Konovalov, Appl. Phys. Lett. **80**, 410 (2002).
[15] R. C. Clarke and J. W. Palmour, Proc. IEEE **90**, 987 (2002).
[16] J. R. Jenny, S. G. Müller, A Powell, V. F. Tsvetkov, H. McD. Hobgood, R. C. Glass, and C. H. Carter, J. Electron. Mater. **31**, 366 (2002).
[17] T. T. Petrenko, T. L. Petrenko, V. Y. Bratus, and J. L. Monge, Physica B **308–310**, 637 (2001).
[18] A. v. Duijn-Arnold, T. Ikoma, O. G. Poluektov, P. G. Baranov, E. N. Mokhov, and J. Schmidt, Phys. Rev. B **57**, 1607 (1998).
[19] S. Greulich-Weber, Phys. Status Solidi A **210**, 415 (1998).
[20] M. Bockstedte, A. Mattausch, and O. Pankratrov, Mater. Sci. Forum **353–356**, 447 (2001).
[21] A. Zywietz, J. Furthmuller, and F. Bechstedt, Phys. Rev. B **59**, 15 166 (1999).
[22] L. Torpo, M. Marlo, T. E. M. Staab, and R. M. Nieminen, J. Phys.: Condens. Matter **13**, 6203 (2001).